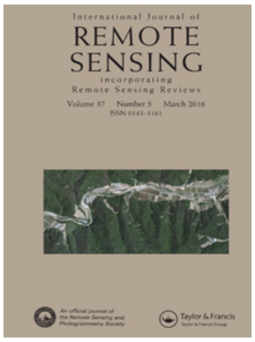

International Journal of Remote Sensing

ISSN: 0143-1161 (Print) 1366-5901 (Online) Journal homepage: https://www.tandfonline.com/loi/tres20

Mapping riparian habitat using a combination ofremote-sensing techniques

Seung Gyu Jeong, Yongwon Mo, Ho Gul Kim, Chong Hwa Park & Dong Kun Lee

INTERNATIONAL JOURNAL OF REMOTE SENSING, 2016
VOL. 37, NO. 5, 1069–1088
http://dx.doi.org/10.1080/01431161.2016.1142685

Taylor & Francis
Taylor & Francis Group

OPEN ACCESS

Mapping riparian habitat using a combination of remote-sensing techniques

Seung Gyu Jeong[a], Yongwon Mo[b], Ho Gul Kim[b], Chong Hwa Park[c] and Dong Kun Lee[a,d]

[a]Research Institute of Agriculture and Life Sciences, Seoul National University, Seoul, Republic of Korea; [b]Interdisciplinary Program in Landscape Architecture, Seoul National University, Seoul, Republic of Korea; [c]Department of Landscape Architecture, Graduate School of Environmental Studies, Seoul National University, Seoul, Republic of Korea; [d]Department of Landscape Architecture & Rural System Engineering, College of Agriculture Life Sciences, Seoul National University, Seoul, Republic of Korea

ABSTRACT

Light detection and ranging (lidar) and object-oriented classification (OOC) can be used to overcome the shortcomings of the traditional pixel-based classification (PBC) of coarse spatial resolution data, such as Landsat data, for habitat mapping in riparian zones. The purposes of this study were to investigate methods to classify multispectral data and lidar for riparian habitat mapping, and to identify major habitat components for two target species. The mapping of riparian habitat based on OOC and Decision Tree Classification (DTC) was carried out by merging vertical data from lidar and spectral data of high-resolution imagery. Our results showed an overall classification accuracy of 88.2%. In particular, small and continuous habitat types, such as short and tall grasses, rock outcrop and gravel, and riffles, improved the classification accuracy compared with the pixel-based methods. The habitat patches and paths for each target species were identified by incorporating the point data from the field survey and the outcomes of image classification. Our study demonstrated that the proposed methodology can be successfully used for the identification and restoration of fragmented riparian habitats, and can offer an opportunity to obtain high classification accuracies for micro-habitat components in dynamic riverine areas.

ARTICLE HISTORY
Received 2 January 2015
Accepted 2 January 2016

1. Introduction

Riparian zones act as an important interface between aquatic and terrestrial ecosystems (Naiman and Décamps 1997), and provide ecological corridors for the migration of wildlife (Hilty and Merenlender 2004; Rodriguez-Iturbe et al. 2009). Most of the natural water resources in the world have been modified owing to the construction of human artefacts, including dams and embankments for flood control and the development of water resources. Riparian areas in the most developed countries have been transformed for agricultural, industrial, or urban uses. Most of the riparian wildlife habitats have been

CONTACT Dong Kun Lee dklee7@snu.ac.kr

destructed and fragmented, and consequently, biodiversity in riparian areas is declining at a fast pace.

In Korea, stream restoration projects that include riparian habitat conservation have been initiated recently. For the systematic planning and management of such conservation projects in any region, it is important to know the specific habitat types and their uses (Rodríguez et al. 2003; Saura and Pascual-Hortal. 2007; Melese et al. 2014). However, it is nearly impossible to acquire detailed riparian habitat data through field surveys because of the large requirements in terms of resources (Marcus et al. 2002). Therefore, detailed riparian ecological surveys on a wide extent would be a financial burden to most environmental agencies.

Remote sensing can be used for the habitat mapping of a dynamic landscape at a high level of detail and spatial distribution. Most previous habitat mapping projects that used remote sensing focused on the classification of broad habitat types such as forests, grasslands, wetlands, and bare soil from the perspective of land-cover classification (Bevanda et al. 2014; Corbane et al. 2015), and ranged from high spatial resolution (Quickbird) (Keramitsoglou et al. 2005; Ke, Quackenbush, and Im 2010) to medium spatial resolution (Landsat Thematic Mapper) (Bock et al. 2005; Tiede et al. 2010). However, mapping at these resolutions might not provide accurate results in terms of discrimination at the individual species level because riparian areas have high land-cover heterogeneity and small patch sizes (Kalliola and Syrjänen 1991; Smith et al. 2002). In the classification process, traditional pixel-based approaches based on extremely high resolutions have resulted in 'salt and pepper' effects (Ke, Quackenbush, and Im 2010), and failed to delineate actually habitat boundaries because they are based on the spectrum information of each individual pixel. Thus, these approaches would be insufficient to delineate continuous habitat boundaries and components, or to identify habitat characteristics based on the species-level requirements (Pekkarinen 2002; Hall et al. 2009).

A detailed habitat-type mapping for the selected target species is important to understand the meticulous spatial patterns of habitats and to identify the heterogeneous ecological structures (Borcard and Legendre 2002; Engler, Guisan, and Rechsteiner 2004; Gottschalk et al. 2011). Such habitat characteristics have been used to associate the presence, species richness, and dispersal paths of wildlife, and to infer the specific characteristics of habitats through which various organisms are associated based on their ecological requirements (Melese et al. 2014). However, as mentioned earlier, fine-scale habitat mapping is still challenging in riparian zones because of their high spatial variability and limited widths (Congalton et al. 2002; Varela et al. 2008; Fernandes, Aguiar, and Ferreira 2011; Corbane et al. 2015). Hence, in most cases, habitat mapping using remote sensing would focus on the classification of terrestrial vegetation covers (Bork and Su 2007; Gilmore et al. 2008; Hellesen and Matikainen 2013). The extraction of small and complex microhabitat components in dynamic riverine areas is, thus, a challenging task (Rapinel, Hubert-Moy, and Clément 2014).

The employment of Object-Oriented Classification (OOC) and light detection and ranging (lidar) with Decision Tree Classification (DTC) could help overcome the shortcomings of the traditional approaches. A detailed classification of the riparian habitat types can be obtained through this approach since image objects can be characterized through thematic or continuous information based on polygons from ancillary data rather than the pixel-based approach based only on a single piece of spectral information (Qian, Zhou, and Hou 2007; Dehvari and Heck 2009). Furthermore, lidar offers quite detailed vertical measurements that can be used to characterize vegetation strata, which are significant habitat components. Biological characteristics such as the height and biomass of large trees and canopy closure as well as various physical characteristics such as types of substrates, rock outcrops, and stream flows can be measured (Hyde et al. 2006; Rapinel, Hubert-Moy, and Clément 2014). This approach should be sufficient for presenting a detailed overview of the riparian habitats boundaries, components, and characteristics. Thus, the objectives of this study were to investigate methods to apply multispectral data and lidar for riparian habitat mapping, and to identify major habitat patches and paths essential to the conservation of the selected target species.

2. Materials and methods

2.1. *Study site*

The study site is a part of the Seom River watershed near the town of Hoengseong, Gangwon-do, South Korea (Figure 1). The site is characterized by high biodiversity and has suitable habitats for some protected and endangered wildlife species such as otters (*Lutra lutra*), leopard cats (*Felis bengalensis euptilura)*, and water deer (*Hydropotes inermis*). This riparian zone is very important as a part of the main ecological axis of the aquatic ecosystem of South Korea. Dominant riparian tree species are black locust (*Robinia pseudoacacia)*, rose gold pussy willow (*Salix gracilistyla)*, runner reed *(Phragmites japonica)*, and amur silver-grass (*Miscanthus sacchariflorus*). However, the riparian ecosystems in this region have been facing intensive disturbances from the measures related to flood control, irrigation, and reclamation for agricultural and urban development. Some of the recent stream restoration projects include the construction of bike trails and riverine recreational sites. Although our study site covers an area of only approximately 5 km, it is large enough to encompass the territories of our target wildlife species, and offers diverse land covers for grazing and migrating of the riparian wildlife adjacent to a rural township in a densely populated and quickly urbanizing country.

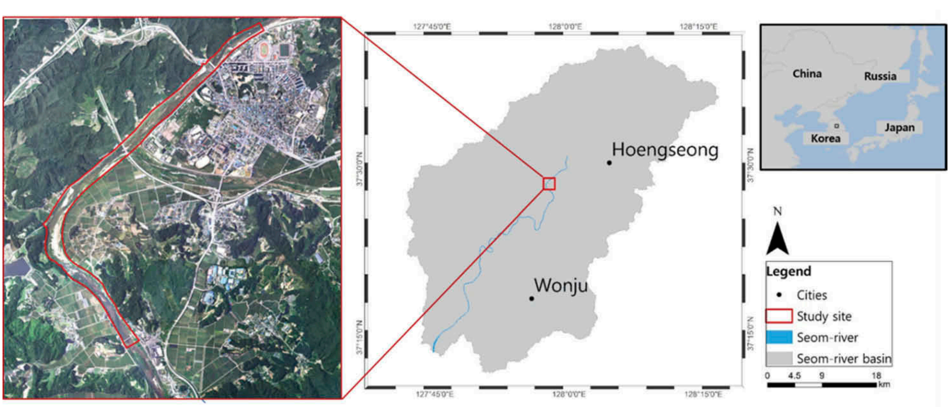

Figure 1. Study site.

2.2. *Target wildlife species and habitat component selection*

It is important to accurately define and identify species-specific habitat components in order to explain species distribution (Xiaofeng et al. 2011). In this study, the selected target species were the Eurasian otter (*Lutra lutra*) and water deer (*Hydropotes inermis*). The otter is a flagship threatened species, and is also one of the key species in riparian ecosystems (Stevens, Organ, and Serfass 2011; Scorpio et al. 2014); their range covers most of Europe and Asia and can be a useful indicator for the evaluation of ecological disturbances or for conservation planning (Soulé and Terborgh 1999). White, McClean, and Woodroffe (2003) showed that habitat types associated with spraints and not the density and height of vegetation affect the otter's habitat characteristics. Furthermore, Ruiz-Olmo, López-Martín, and Palazón (2001) discuss the flow regime and relationships with otter abundance and its food.

The water deer is considered an important wildlife species across the world because it is not particularly adaptable and appears to be rather sensitive to environmental changes. They inhabit mainly the downstream of the Yangtze River in China and the Korean Peninsula (Kim et al. 2011). However, the size of their population has been continuously declining because of anthropogenic activities such as poaching and habitat destruction (Harris and Duckworth 2010). Rhim and Lee (2007) showed that habitat type associated with tracking route and hydrophytes, tall grasses, shrubs along the riparian corridors, and shrubs and small trees in uphill forests affect the habitat characteristics of the water deer. Furthermore, Kim et al. (2011) reported the preferred grazing and hide covers of the water deer to be dense grass and reeds, often on shrubby slopes and riparian forests. Thus, we could conclude that important habitat components for our target species were: *Robinia, Salix*, tall grass, and short grass as the main vegetation types; gravel, gravel/sand, sand, and rock outcrop as substrates; and riffles and pools under waterbodies.

2.3. *Field survey and accuracy assessment*

Field data necessary for verifying the classification accuracy were collected by using the stratified random sampling method during April–September 2011. The sampling method was demonstrated to have a higher accuracy than the simple random sampling method for use with DTC (Borak 1999; Laliberte, Fredrickson, and Rango 2007). The sample size per class was set to a minimum of 50 points based on Congalton (1991) recommendations, with a total of 678 samples. The number of samples collected through field surveys and visual interpretation of aerial photographs were 260 and 418, respectively. The accuracy of the OOC in this study was calculated using the error matrix. This method allows the calculation of specific accuracies such as the overall, producer's, and user's accuracies using the kappa coefficient (Congalton 1991). The vertical accuracy of the Canopy Height Model (CHM)-extracted lidar was assessed using a linear regression model and a field survey employing a laser range finder and a prism pole for vegetation types, rock outcrops, and artificial objects.

The data including the traces of wildlife (footprints and excrements) and tracked routes were collected during the entire study period from April 2011 to February 2014.

Chi-square and Mann–Whitney tests were used to identify the relationships among the various habitat-use patterns identified.

2.4. *Image data and preprocessing*

Lidar and spectral data consisting of high-resolution imagery of Color Infrared (CIR) band acquired in May 2009 were used in this study. The CIR wavelength ranged from 500 to 900 nm, and was divided into green (500–530 nm), yellow (530–580 nm), orange (580–630 nm), red (630–700 nm), and Near Infrared (NIR, 700–900 nm) bands. The imagery had a 12-bit radiometric depth, with spatial resolution of 0.12 m and 0.2 m, respectively, for the three visible bands and the NIR band. The imagery was ortho-rectified using a bilinear interpolation resampling method based on the National Geographic Accuracy Standards (NGAS). All points tested for the imagery were from 0.2 to 0.3 cm of mean error for the x and y coordinates, and within 0.6 cm mean error for the z coordinate. Lidar data were recorded for the first and last returns for each laser pulse, with an average point spacing of 4.88 per m^2 (maximum 6.41, minimum 3.29). Lidar height values were extracted using the natural neighbour interpolation method.

2.5. *OOC and decision tree*

The OOC was performed by multi-resolution segmentation of the images using eCognition V8.4 software. The basic concept is to group and divide the adjacent pixels by means of segmentation based on three parameters: scale, shape/colour, and smoothness/compactness (Baatz and Schäpe 2000). The segmentation of the image data is considered the most important process in extracting boundaries of the dominant objects (Hall et al. 2004; Mallinis et al. 2008). The scale parameter determines the average size of objects based on maximum heterogeneity in each segment. The shape/colour and smoothness/compactness parameters can be weighted from 0 to 1. Higher values of shape would decrease the influence of colour in the segmentation process. Smoothness and compactness define the shape of the edge of the complex. Higher compactness values will generate more boundaries with heterogeneous shapes. Typically, a proper combination of weighting parameters is selected by trial and error methods for the successful extraction of objects and complex boundary of the riparian vegetation (Moffett and Gorelick 2013; Jeong and Park 2013).

Initially, we used a multi-resolution segmentation algorithm with a scale parameter of 80, 50, and 30 at each segmentation step as shown in Table 1. The final selection of scale parameters was determined through visual inspection of the segmentation. A successful segmentation would result in the identification of heterogeneous land covers and the creation of a hierarchical network of image objects (Laliberte, Fredrickson, and Rango 2007). The weightings for the colour and compactness parameters were set at 0.9, based

Table 1. Multi-resolution setting used for segmentation parameters.

Segmentation	Scale parameter	Colour/Shape	Smoothness/Compactness
Level 1	80	0.9/0.1	0.1/0.9
Level 2	50	0.9/0.1	0.1/0.9
Level 3	30	0.9/0.1	0.1/0.9

on segmentation testing. Finally, the labels for cover types were determined using the nearest neighbour classification algorithm.

2.6. *DTC*

This study employed DTC with ancillary data for each class using the multi-resolution segmentation stage and nearest neighbour classification. DTC has been demonstrated to yield improved classification accuracies over the traditional classifiers (Hansen, Dubayah, and DeFries 1996; Pal and Mather 2003) for mapping wetland mosaic habitats (Simard et al. 2002; Bwangoy et al. 2010). In particular, small patches were relatively easy to extract and the classification accuracies were comparable to other classification techniques (Patil and Bichkar 2006). Moreover, DTC incorporating ancillary data can improve the classification accuracy for land covers by adjusting iteratively the decision rules for the problematic classes (Treitz and Howarth 2000; Laliberte et al. 2006).

As shown in Table 2, the ancillary data used in our study for the thresholds criteria in the OOC and DTC stages included normalized difference vegetation index (NDVI), brightness channels, CHM, and digital elevation model (DEM). The NDVI has been widely used as a variable for vegetational analyses (Norman 2012), and was reported to be effective for substrate classification in highly heterogeneous areas (Behbahni et al. 2010; Ghorbani, Mossivand, and Ouri 2012). Brightness channels are highly sensitive to topography because they are related to soil moisture (Ivits and Koch 2002; Lu et al. 2004; Pierce, Farris, and Taylor 2012). Thus, brightness channels could be useful for classifying substrates into gravel, sand, and rock outcrops in the stream channel. The CHM has also demonstrated to improve the classification accuracy of grasses, shrubs, and trees in wetland or riparian areas (Goodwin, Coops, and Culvenor 2006). Thus, DTC using ancillary data should be based on the expert knowledge on riparian habitats and paths.

The decision classification process, cluster separation, and specific criteria are shown in Figures 2 and 3. The first stage is classifying the vegetation, substrate, and water surface. The thresholds of NDVI for the extraction of vegetation, substrate, and water ranged from 1 to −1. The range of NDVI values for shrubs and grass was from 0.2 to 0.3. The NDVI values of gravel, sand, and rock were set to be 0.1 or less (Carlson and Ripley 1997; Chander and Markham 2003). Low NDVI values correspond to rock and sand, and moderate values to shrubs and grasslands in the scatter plot, as shown in Figure 2(*b*).

The second stage involves subdividing the vegetation into tree and ground cover using CHM. The class of tree was also separated into *Salix* and *Robinia* based on DEM. Ground cover was subdivided into tall grass and short grass based on CHM in the scatter plot, as

Table 2. Habitat variables used in this study.

Variable (abbreviated)	Variable (expanded)	Description
NDVI	Normalized difference vegetation index	Pixel calculation based on the ratio formulations between red and near infrared wavelengths. The value ranged from −1 to 1.
CHM	Canopy Height Model	Digital elevation model (DEM) values subtracted from the Digital surface model (DSM).
Brightness	Brightness	Sum of mean values in all bands divided by the number of bands.
DEM	Digital elevation model	Ground elevation value derived from lidar.
DSM	Digital surface model	Surface elevation value derived from lidar.

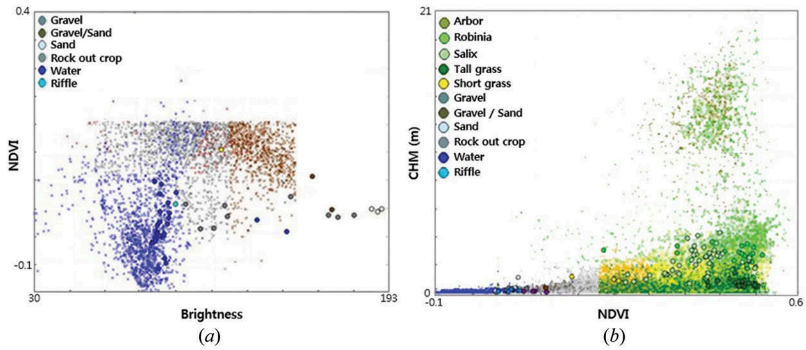

Figure 2. Cluster separation in scatter plots: (*a*) cluster separation: brightness and NDVI and (*b*) cluster separation: CHM and NDVI.

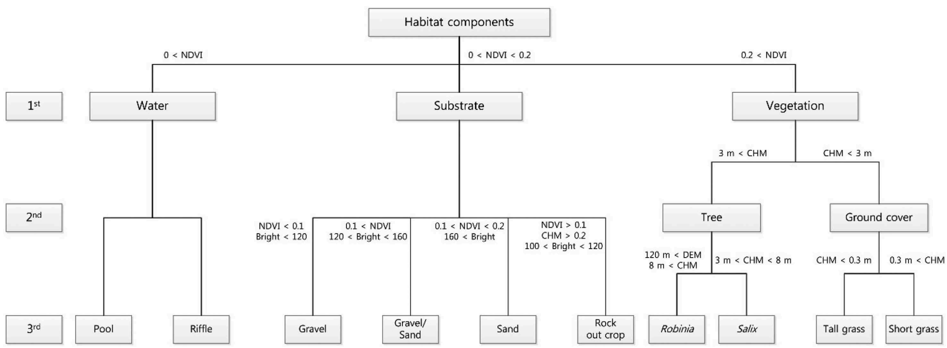

Figure 3. Criteria and stages for the decision tree.

shown in Figure 2(*b*). The height threshold for the classification of tall grass and grass is 0.3 m. Finally, the substrates were further subdivided into gravel, gravel/sand, sand, and rock outcrops using both NDVI and brightness in scatter plots shown in Figure 2(*a*). In particular, rock outcrops in stream channel were extracted using variables of NDVI, CHM, and brightness. The outcomes of our riparian habitat components are shown in Figure 3. There are three major categories (vegetation, substrate, water) and 10 subcategories (*Robinia, Salix*, tall grass, short grass, gravel, gravel/sand, sand, rock outcrop, riffle, and pool).

3. Results

The results and the accuracy of the CHM are shown in Figure 4. The R^2 of 0.99 of the linear model between the CHM and field-measured heights is characterized by very high accuracy, as shown in Figure 4(*b*). The heights of artefacts and rock outcrops in stream channels showed better agreement than those of the trees. The first return in lidar measurements often collects data from the shoulder or understorey of trees instead of the top (Nelson, Krabill, and Tonelli 1988; Rönnholm et al. 2004). Thus, the CHM tends to underestimate the tree height relative to other objects. These results show that the CHM can be employed for our riparian mapping.

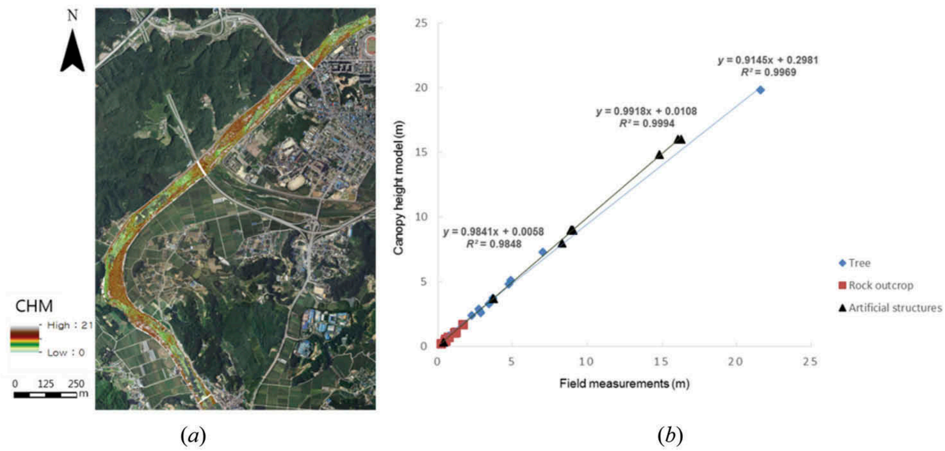

Figure 4. (*a*) Canopy height model map, (*b*) comparison between the CHM obtained from lidar (y axis) and the field measurements (*x* axis).

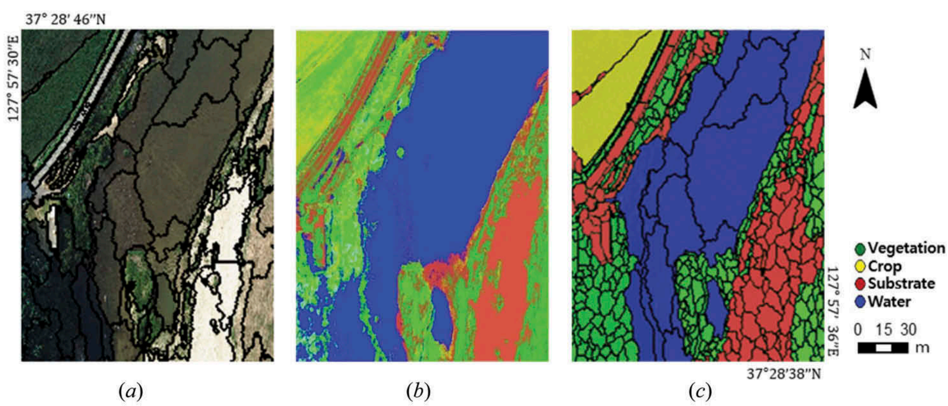

Figure 5. A comparison of the classification results. (*a*) Segmentation, (*b*) PBC (ISODATA), and (*c*) OOC.

The result of the multi-resolution image segmentation is shown in Figure 5. The boundaries of homogeneous objects, such as vegetation, substrate, and waterbody, were precisely delineated, which shows few salt and pepper patterns compared to those of pixel-based classification (PBC). In particular, the NDVI threshold of 0.2 for the segmentation could successfully differentiate the vegetation patches from the substrate on embankments, as shown in Figure 6(*b*). Figure 7(*c*) shows that the height value of the OOC using CHM effectively differentiated tall grass and short grass despite the similar spectral values compared with the results of PBC (Figure 7(*a*)) and OOC (Figure 7(*b*)). Consequently, Figures 6 (*b*) and 7(*c*) show that approaches based on OOC with ancillary data such as CHM and NDVI generated better outcomes in terms of the classification accuracy and the successful delineation of continuous boundaries than the classification using only spectral information. As shown in Figure 8, the application of OOC with a decision tree could successfully classify similar covers such as gravel, gravel/sand, and

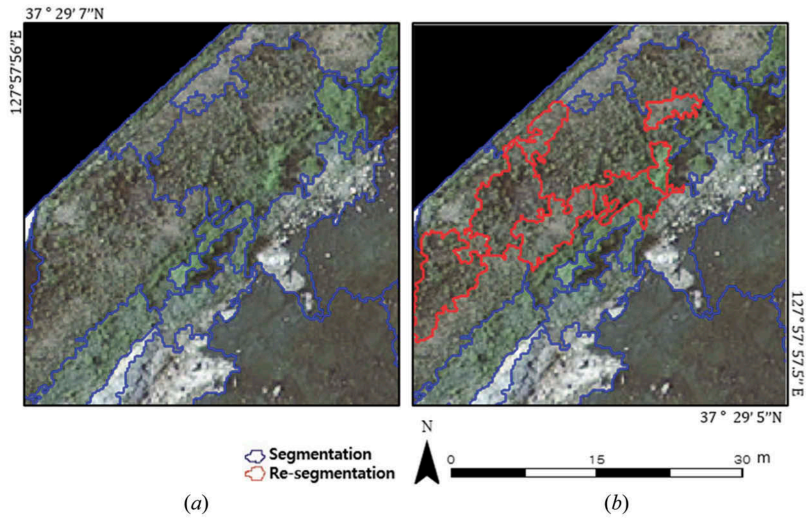

Figure 6. A comparison of the segmentation results for embankments: (*a*) level 1 segmentation and (*b*) re-segmentation with NDVI.

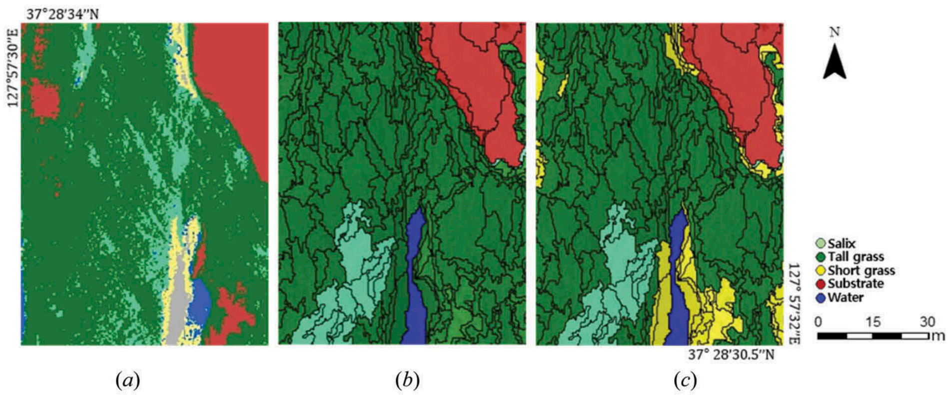

Figure 7. A comparison of the classification results: (*a*) PBC (maximum likelihood), (*b*) OOC, and (*c*) OOC with CHM.

sand using threshold NDVI and brightness values in the range 0–0.2 and 70–170, respectively. The parameter ranges were obtained from their scatter plots.

Figure 9(*a*) shows a typical PBC result, and Figure 9(*b*) shows that a classification based on OOC is not sufficient to extract rock outcrops in a stream channel, which have positive NDVI values and values higher than water surfaces in the scatterplot. Thus, Figure 9(*c*) shows that they can be correctly extracted from the water surface based on two conditions: positive NDVI and CHM mean values greater than 20 cm. Rock outcrops and gravel can also be separated easily because the brightness values of the former are higher than those of the latter. Figure 10 shows the difference of OOC and PBC for the classification of a complex stream bed that is likely to include rock outcrop, pool, and riffle.

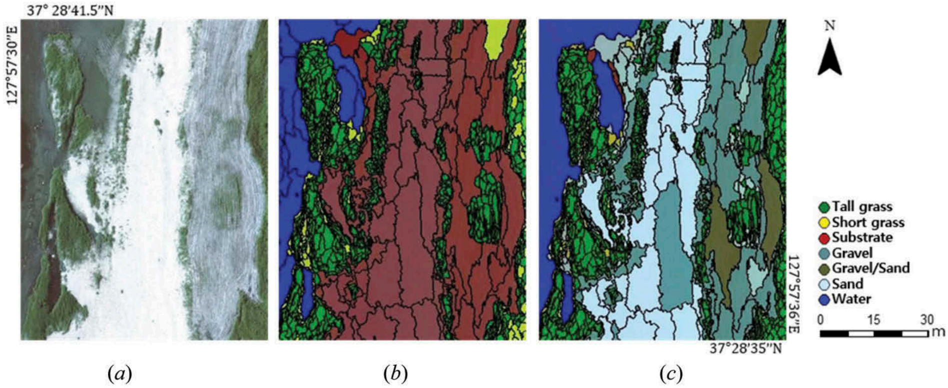

Figure 8. A comparison of the classification results: (*a*) raw data, (*b*) OOC, and (*c*) OOC with NDVI and brightness.

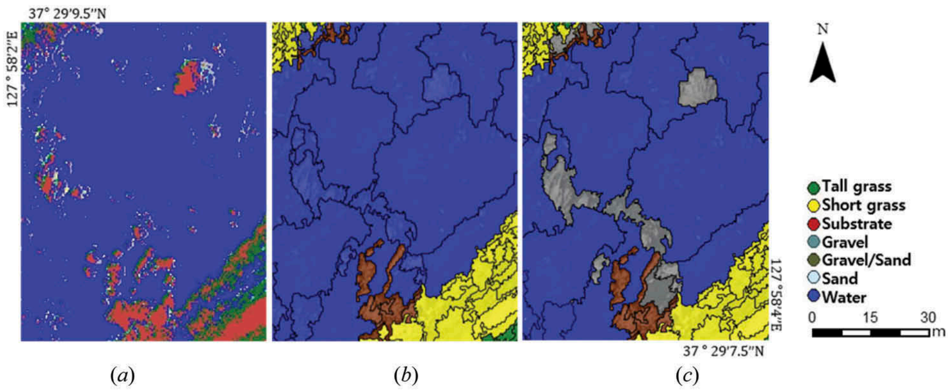

Figure 9. A comparison of the classification results: (*a*) PBC (maximum likelihood), (*b*) OOC, and (*c*) reclassification with CHM and brightness.

Figure 10(*b*) shows that PBC results in a salt and pepper mixture of rock outcrops and waterbodies. However, Figure 10(*c*) shows that riffles could be extracted using brightness, NDVI, and CHM. Riffles are stream segments characterized by the relatively fast flow velocity compared with adjacent waterbodies due to their narrow and shallow shapes. Three criteria were used for riffle extraction: brightness values similar to gravel, CHM values higher than those of water, and negative and positive NDVI values for the mixed areas of waterbodies. Figures 9(*c*) and 10(*c*) show that OOC with ancillary data such as CHM and brightness resulted in better outcomes than that of PBC for the classification of small objects, such as rock outcrops and gravel in riffles, and for the representation of objects with continuous forms, such as riffles. Furthermore, this method showed that the ‘salt and pepper effect’ is reduced in the high-resolution images resulting from the ambiguity of the statistical definition.

The results and the accuracy of the riparian habitat mapping using combinations of remote-sensing techniques are shown in Table 3 and Figure 11. This classification approach has consistently yielded better results with the classification accuracies

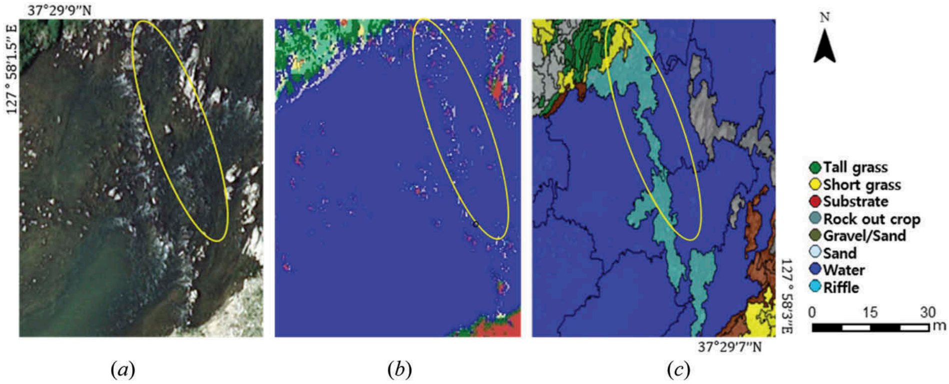

Figure 10. A comparison of the classification results for riffles: (*a*) aerial imagery, (*b*) PBC, (*c*) OOC with NDVI, CHM, and brightness.

Table 3. Confusion matrix and accuracy assessment for the classification based on the DTC with OOC.

	Robinia	*Salix*	Tall grass	Short grass	Gravel	Gravel/ Sand	Sand	Rock outcrop	Riffle	Producer's accuracy (%)	User's accuracy (%)
Robinia	54	3	0	0	0	0	0	0	0	90	94
Salix	4	60	0	0	0	0	0	0	0	90	93
Tall grass	2	3	89	3	0	0	0	0	0	89	91
Short grass	0	0	9	76	1	2	1	0	0	86	85
Gravel	0	0	0	0	51	0	3	2	1	86	89
Gravel/ Sand	0	0	1	8	3	100	7	4	2	86	80
Sand	0	0	0	0	2	13	64	1	0	85	80
Rock outcrop	0	0	0	0	0	0	0	57	2	89	96
Riffle	0	0	0	1	2	0	0	0	47	90	94
Total	60	66	99	88	59	115	75	64	52		

Overall accuracy = 88.2; Kappa coefficient = 0.86

ranging from 80% to 96%. The overall classification accuracy and kappa coefficient were 88.2% and 0.86, respectively. The accuracy satisfies the standard proposed by many researchers (Fielding and Bell 1997; Bock et al. 2005). Both producer's and user's accuracies of all of the classes were higher than 80%. The results of classes are shown in Table 3. The *Robinia* and *Salix* trees were accurately identified because of their distinct reflectance and height, as can be seen in their scatter plots (Figure 2). Since *Robinia* was mainly distributed on the vegetated embankments, it could be classified easily using slope and CHM. The classification accuracy was relatively lower for classes such as gravel, gravel/sand, and sand. The rock outcrops were also identified with even higher accuracy because they could be easily separated using CHM, brightness, and NDVI (Figure 8). Gravel/sand and sand were identified with relatively lower accuracy because of similar brightness thresholds (Figure 2 (*a*). Riffles, on the other hand, were identified with high accuracy because of their higher NDVI and brightness values compared with calm water surfaces, and thus they could be grouped as homogeneous polygons in the

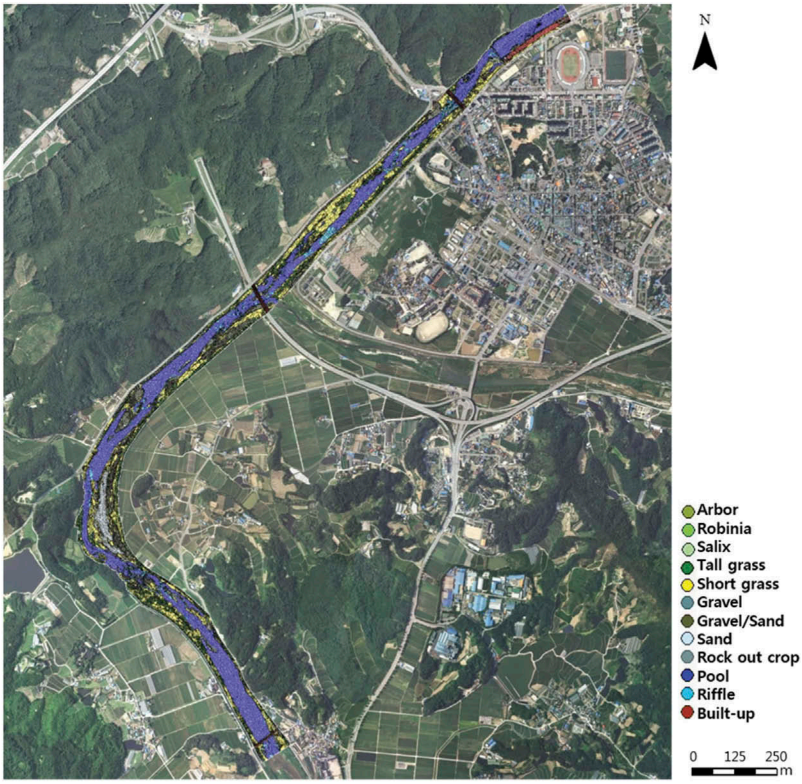

Figure 11. Habitat component classification.

segmentation process. Only a few misclassifications were observed within the classes, e.g. between gravel and sand/gravel, and between tall grass and short grass.

The habitat-use patterns of water deer are shown in Figure 12(*a*) and Table 4. The various land-cover types obtained through the field survey of footprint and faecal trace and snow tracking were 80 points and 50 points, respectively. The longitudinal slope of the water deer tracking route ranged from 0° to 20°, and the average slope was 14.32°. The CHM of the route ranged from 0.2 m to 8 m, and the average CHM was 0.46 m. The paths preferred by water deer were characterized by three factors: a longitudinal slope of less than 15°, the presence of vegetation with a CHM of 0.2–1.0 m, and the land cover of tall grass, short grass, gravel & sand, and sand (Slope and CHM, Mann–Whitney test, $p < 0.01$; land cover, χ^2 test, $p < 0.01$; Table 4). Meanwhile, the mean values of slope and CHM in habitat patches were 7.41 and 0.80 m, respectively. They show different patterns of habitat use as paths and habitat (χ^2 test, $p < 0.01$; Table 4). The path points tend to have a higher mean slope and lower CHM than the habitat points (Slope, CHM, Mann–Whitney test, $p < 0.01$). Figure 12(*a*) shows that habitat-use patterns can be mapped as path and habitat patches.

The habitat patterns of otter, investigated through the analyses of 20 sampling points collected through a field survey of footprint, faecal materials, and sprints, can be summarized as shown in Table 5. The range of CHM of an otter was from 0 m to 12 m, and the average CHM was 0.12 m (CHM, Mann–Whitney test, $p < 0.01$; Table 5).

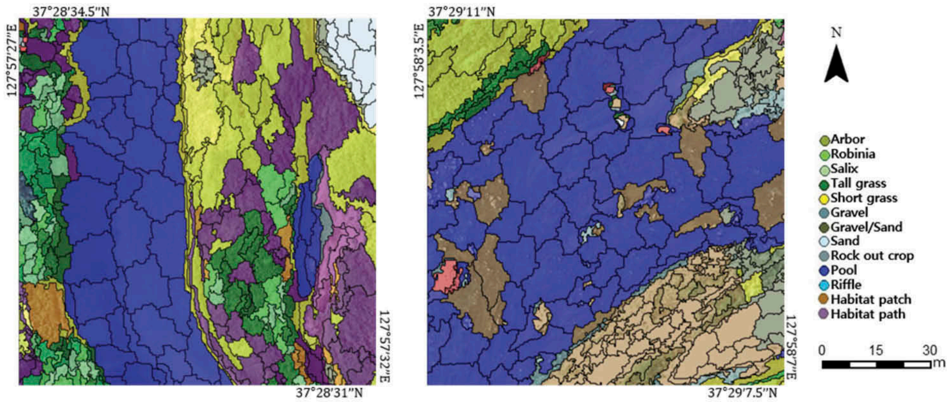

(*a*) (*b*)

Figure 12. Habitat mapping as habitat patches and paths. (*a*) Habitat patches and paths of water deer and (*b*) habitat patches for otter.

Table 4. Occurrence frequency of the Korea water deer from the field survey in the Seom River.

Species	Habitat components	Category	Occurrence frequency (%)	
			Habitat patches	Paths
Water deer	Land cover	Robinia	7	13
		Salix	23	9
		Tall grass	40	13
		Short grass	23	39
		Gravel	7	1
		Gravel/sand		21
		Sand		3
		Riffle		1
	Vegetation height (cm)	<20	40	1
		21–40	33	47
		41–60	6	27
		61–80	4	19
		81–100	3	3
		>100	14	3
	Slope (°)	0–5	6	0
		5–10	66	21
		10–15	16	32
		15–20	8	19
		20–25	2	15
		>25	2	13

Note: Significant differences in water deer spotted between patches and paths, χ^2, $p < 0.01$, Mann–Whitney test, $p < 0.01$.

The land-cover types preferred by the otter include gravel/sand, rock outcrop, and short grass (Chi-square test, $p < 0.01$; Table 5). The classification results (Figure 12(*b*)) closely match the segmentation of the otter suitability factor such as sand, rock outcrop, and riffle.

4. Discussion

The results demonstrated that OOC, applied on lidar and high-resolution images, is more effective in classifying the detailed riparian habitat components at our test site. The

Table 5. Occurrence frequency of the otter from the field survey in the Seom River.

Species	Habitat components	Category	Occurrence frequency (%)
			Habitat patches
Otter	Land cover	Short grass	31
		Gravel/sand	22
		Sand	10
		Rock outcrop	26
		Riffle	11
	Vegetation height (cm)	<20	5
		21–40	68
		41–60	21
		61–80	6
		81–100	0
		>100	0

Note: Significant difference between the observed and expected habitat type, χ^2, $p < 0.01$, Mann–Whitney test, $p < 0.01$.

overall classification accuracy was 88.2%, which is higher than those reported by Marcus et al. (2002), Chust et al. (2008), Ghioca-Robrecht, Johnston, and Tulbure (2008), and Rapinel, Hubert-Moy, and Clément (2014). We could achieve a high classification accuracy for small and continuous habitat types, such as short and tall grasses, rock outcrop and gravel, and riffle. Other previous studies in riparian and wetland areas based on the traditional land-cover mapping at a macro or a coarse level could not produce such outcomes (Bock et al. 2005; McKenna Jr and Castiglione 2010; Ouyang et al. 2011; Bargiel 2013; Mücher et al. 2015; Rapinel, Hubert-Moy, and Clément 2014; Corbane et al. 2015). As reported by several researchers (Zhang and Huang 2010; Nie et al. 2010; Hölbling et al. 2012; Tehrany, Pradhan, and Jebuv 2014), the salt and pepper effect for high-resolution data could be reduced significantly. Furthermore, we could identify suitable habitats for two target wildlife species by combining trace data and image classification through OOC and DTC. Wildlife habitats were subsequently classified into grazing habitats and paths for each target species.

The levels of segmentation parameters – scale parameter, colour/shape, smoothness/compactness – could significantly affect the land-cover classification with OOC. The objective of the multi-scale segmentation was to classify the habitat components and delineate the precise boundaries at a micro level. Our results were consistent with the other studies concerning the comparison between OOC and PBC (Radoux and Defourny 2007; Im, Jensen, and Tullis 2008; Ouyang et al. 2011).

The scale parameter of level 1 should be lower than 90; however, when the value was set higher than 90, the segmentation did not adequately delineate the boundaries of riparian vegetation. The small-scale values of 30 were effective to generate the boundaries of vegetation patches, particularly grass and small patches of rock outcrop and gravel within the stream channel. These objects have relatively simple and compact shapes. The edge of the complicated riparian vegetation, such as *Phragmite*, was precisely extracted using a compactness parameter of lower than 0.9, whereas compactness values higher than 0.9 would result in the fringed shapes of boundaries, similar to the results shown by Kloiber et al. (2015).

A colour parameter setting of 0.9 was well-suited for the image segmentation process, which could be further influenced by spectral values as opposed to the shape parameter for riparian land-cover classification (Qian, Zhou, and Hou 2007). This setting was suitable for resolving the problems caused by small differences in the colour of such objects. This means that the colour parameters are more sensitive when CIR images are used as small patches in the algorithm. This is because the CIR imagery can be sensed by both absorption and reflectance in the NIR band that detects significant differences in the vegetation types. The classification accuracy of the riffle was 90.4%, which is better than that of Marcus et al. (2002). In particular, our study presented that segmentations using NDVI were better suited for the extraction of vegetation boundaries from substrates on embankments (Figure 6). It is important to reduce the misclassification by influencing the vegetation stratum (Sébastien Rapinel, Hubert-Moy, and Clément 2014).

First, brightness and NDVI were extremely effective in dividing stream substrates into gravel, gravel & sand, and sand. The classification accuracies of the substrates were similar to those of Campbell (2007), and much higher than other classifications based on most multispectral classification schemes. As can be seen from the scatter plots, the spectral response of such materials could be affected by infrared and brightness characteristics. Todd and Hoffer (1998) reported that the spectral response of a substrate type is closely related to their soil moisture content.

Second, CHM has been useful for the identification of riparian grasses and stream channel topography. Smeeckaert et al. (2013) reported that CHM was a useful parameter for vegetation mapping and stand breaks, and the classification accuracies of tall grass and short grass were 89.9% and 86.3%, respectively. The classification accuracies for riffles and rock outcrop – 90.3% and 89.0%, respectively – were unexpected.

In this study, a few misclassifications have been observed within the classes (Table 3). This could result from the overlapping distribution of pixels at the threshold baseline because of the riparian habitat characterized by strong environmental gradients in the variability in the occurrence of floods. A recent classification algorithm, such as Random Forest, and multi-temporal data could offer the opportunity to obtain a much higher accuracy using a multiple-decision tree and vegetation phenology in riparian areas.

5. Conclusion

The purpose of this study was to produce detailed riparian habitat maps for selected wildlife species by using ancillary data of the study area. We investigated ways to combine the high-resolution spectral data and lidar as well as to classify the riparian habitats and potential corridors to connect the fragmented habitats in highly developed stream corridors. The outcomes of this study extend those of most previous studies usually focused on broad habitat types, coarse-scale classification based on only spectral data and PBC, and consequently had difficulty in capturing the continuous and multidimensional habitat features at dynamic landscapes such as urban streams. The outcomes of the study can be summarized as follows. First, the combination of high-resolution spectral data and lidar for the extraction of environmental factors provided the basis for the riparian habitat classification in terms of ecology. Second, OOC using ancillary data such as NDVI, CHM, brightness, and DEM could accurately extract stream substrates and continuous habitat types. In particular, small patches, such as sand, gravel, rock outcrop, and short and tall grasses, were classified at overall classification accuracies of 88.2%. Third, the optimum combinations of segmentation parameters of scale, colour/shape, and smoothness/compactness could be achieved using the field survey results. Finally, the land-cover classification could be transformed to riparian habitat maps that include habitat patches and paths for two target species of otter and water deer. These maps could be essential to habitat restoration in the urbanized stream corridors.

Disclosure statement

No potential conflict of interest was reported by the authors.

Funding

This work was supported by the Korea Environmental Industry and Technology Institute (KEITI) [grant number 416-111-014]; the KEITI [grant number 2014-001-310007]; and the BK 21 Plus Project in 2015 (Seoul National University Interdisciplinary Program in Landscape Architecture, Global leadership programme towards innovative green infrastructure).

Reference

Baatz, M., and A. Schäpe. 2000. “Multiresolution Segmentation: An Optimization Approach for High Quality Multi-Scale Image Segmentation.” *Angewandte Geographische Informationsverarbeitung* XII: 12–23.

Bargiel, D. 2013. “Capabilities of High Resolution Satellite Radar for the Detection of Semi-Natural Habitat Structures and Grasslands in Agricultural Landscapes.” *Ecological Informatics* 13: 9–16. doi:10.1016/j.ecoinf.2012.10.004.

Behbahni, N., S. S. R. Falah, J. Farzadmehr, S. Y. Erfanifard, and G. M. Ramezani. 2010. “Using Vegetation Indices of ASTER-L1B Imagery to Estimate Single Trees Crown Cover in Arid Rangelands, Case Study; Tag-Ahmadshahi, Southern of Khorassan.” *Rangeland* 4 (1): 93–103.

Bevanda, M., N. Horning, B. Reineking, M. Heurich, M. Wegmann, and J. Mueller. 2014. “Adding Structure to Land Cover–Using Fractional Cover to Study Animal Habitat Use.” *Movement Ecology* 2 (1): 26. doi:10.1186/s40462-014-0026-1.

Bock, M., P. Xofis, J. Mitchley, G. Rossner, and M. Wissen. 2005. “Object-Oriented Methods for Habitat Mapping at Multiple Scales–Case Studies from Northern Germany and Wye Downs, UK.” *Journal for Nature Conservation* 13: 75–89. doi:10.1016/j.jnc.2004.12.002.

Borak, J. S. 1999. “Feature Selection and Land Cover Classification of a MODIS-like Data Set for a Semiarid Environment.” *International Journal of Remote Sensing* 20 (5): 919–938. doi:10.1080/014311699212993.

Borcard, D., and P. Legendre. 2002. “All-Scale Spatial Analysis of Ecological Data by Means of Principal Coordinates of Neighbour Matrices.” *Ecological Modelling* 153 (1–2): 51–68. doi:10.1016/S0304-3800(01)00501-4.

Bork, E. W., and J. G. Su. 2007. “Integrating LIDAR Data and Multispectral Imagery for Enhanced Classification of Rangeland Vegetation: A Meta Analysis.” *Remote Sensing of Environment* 111 (1): 11–24. doi:10.1016/j.rse.2007.03.011.

Bwangoy, J. R. B., M. C. Hansen, D. P. Roy, G. De Grandi, and C. O. Justice. 2010. “Wetland Mapping in the Congo Basin Using Optical and Radar Remotely Sensed Data and Derived Topographical Indices.” *Remote Sensing of Environment* 114 (1): 73–86. doi:10.1016/j.rse.2009.08.004.

Campbell, J. B. 2007. *Introduction to Remote Sensing*. 4th ed. New York: The Guilford Press.

Carlson, T. N., and D. A. Ripley. 1997. “On the Relation between NDVI, Fractional Vegetation Cover, and Leaf Area Index.” *Remote Sensing of Environment* 62 (3): 241–252. doi:10.1016/S0034-4257(97)00104-1.

Chander, G., and B. Markham. 2003. "Revised Landsat-5 TM Radiometric Calibration Procedures and Postcalibration Dynamic Ranges." *IEEE Transactions on Geoscience and Remote Sensing* 41 (11): 2674–2677. doi:10.1109/TGRS.2003.818464.

Chust, G., I. Galparsoro, Á. Borja, J. Franco, and A. Uriarte. 2008. "Coastal and Estuarine Habitat Mapping, Using LIDAR Height and Intensity and Multi-Spectral Imagery." *Estuarine, Coastal and Shelf Science* 78 (4): 633–643. doi:10.1016/j.ecss.2008.02.003.

Congalton, R. G. 1991. "A Review of Assessing the Accuracy of Classifications of Remotely Sensed Data." *Remote Sensing of Environment* 37 (1): 35–46. doi:10.1016/0034-4257(91)90048-B.

Congalton, R. G., K. Birch, R. Jones, and J. Schriever. 2002. "Evaluating Remotely Sensed Techniques for Mapping Riparian Vegetation." *Computers and Electronics in Agriculture* 37 (1–3): 113–126. doi:10.1016/S0168-1699(02)00108-4.

Corbane, C., S. Lang, K. Pipkins, S. Alleaume, M. Deshayes, V. E. G. Millán, T. Strasser, J. V. Borre, S. Toon, and F. Michael. 2015. "Remote Sensing for Mapping Natural Habitats and Their Conservation Status - New Opportunities and Challenges." *International Journal of Applied Earth Observation and Geoinformation* 37: 7–16. doi:10.1016/j.jag.2014.11.005.

Dehvari, A., and R. J. Heck. 2009. "Comparison of Object-Based and Pixel Based Infrared Airborne Image Classification Methods Using DEM Thematic Layer." *Journal of Geography and Regional Planning* 2 (4): 86–96.

Engler, R., A. Guisan, and L. Rechsteiner. 2004. "An Improved Approach for Predicting the Distribution of Rare and Endangered Species from Occurrence and Pseudo-Absence Data." *Journal of Applied Ecology* 41 (2): 263–274. doi:10.1111/j.0021-8901.2004.00881.x.

Fernandes, M. R., F. C. Aguiar, and M. T. Ferreira. 2011. "Assessing Riparian Vegetation Structure and the Influence of Land Use Using Landscape Metrics and Geostatistical Tools." *Landscape and Urban Planning* 99 (2): 166–177. doi:10.1016/j.landurbplan.2010.11.001.

Fielding, A. H., and J. F. Bell. 1997. "A Review of Methods for the Assessment of Prediction Errors in Conservation Presence/absence Models." *Environmental Conservation* 24 (1): 38–49. doi:10.1017/S0376892997000088.

Ghioca-Robrecht, D. M., C. A. Johnston, and M. G. Tulbure. 2008. "Assessing the Use of Multiseason QuickBird Imagery for Mapping Invasive Species in a Lake Erie Coastal Marsh." *Wetlands* 28 (4): 1028–1039. doi:10.1672/08-34.1.

Ghorbani, A., A. M. Mossivand, and A. E. Ouri. 2012. "Utility of the Normalised Difference Vegetation Index (NDVI) for Land/Canopy Cover Mapping in Khalkhal County (Iran)." *Annals of the Biological Research* 3 (12): 5494–5503.

Gilmore, M. S., E. H. Wilson, N. Barrett, D. L. Civco, S. Prisloe, J. D. Hurd, and C. Chadwick. 2008. "Integrating Multi-Temporal Spectral and Structural Information to Map Wetland Vegetation in a Lower Connecticut River Tidal Marsh." *Remote Sensing of Environment* 112 (11): 4048–4060. doi:10.1016/j.rse.2008.05.020.

Goodwin, N. R., N. C. Coops, and D. S. Culvenor. 2006. "Assessment of Forest Structure with Airborne LiDAR and the Effects of Platform Altitude." *Remote Sensing of Environment* 103 (2): 140–152. doi:10.1016/j.rse.2006.03.003.

Gottschalk, T. K., B. Aue, S. Hotes, and K. Ekschmitt. 2011. "Influence of Grain Size on Species–Habitat Models." *Ecological Modelling* 222 (18): 3403–3412. doi:10.1016/j.ecolmodel.2011.07.008.

Hall, O., G. J. Hay, A. Bouchard, and D. J. Marceau. 2004. "Detecting Dominant Landscape Objects through Multiple Scales: An Integration of Object-Specific Methods and Watershed Segmentation." *Landscape Ecology* 19 (1): 59–76. doi:10.1023/B:LAND.0000018371.43447.1f.

Hall, R. K., R. L. Watkins, D. T. Heggem, K. B. Jones, P. R. Kaufmann, S. B. Moore, and S. J. Gregory. 2009. "Quantifying Structural Physical Habitat Attributes Using LIDAR and Hyperspectral Imagery." *Environmental Monitoring and Assessment* 159 (1–4): 63–83. doi:10.1007/s10661-008-0613-y.

Hansen, M., R. Dubayah, and R. DeFries. 1996. "Classification Trees: An Alternative to Traditional Land Cover Classifiers." *International Journal of Remote Sensing* 17 (5): 1075–1081. doi:10.1080/01431169608949069.

Harris, R. B., and J. W. Duckworth. 2010. "Hydropotes Inermis." IUCN Red List of Threatened Species Version 2014.3. http://www.iucnredlist.org.

Hellesen, T., and L. Matikainen. 2013. "An Object-Based Approach for Mapping Shrub and Tree Cover on Grassland Habitats by Use of LiDAR and CIR Orthoimages." *Remote Sensing* 5 (2): 558–583. doi:10.3390/rs5020558.

Hilty, J. A., and A. M. Merenlender. 2004. "Use of Riparian Corridors and Vineyards by Mammalian Predators in Northern California." *Conservation Biology* 18 (1): 126–135. doi:10.1111/j.1523-1739.2004.00225.x.

Hölbling, D., P. Füreder, F. Antolini, F. Cigna, N. Casagli, and S. Lang. 2012. "A Semi-Automated Object-Based Approach for Landslide Detection Validated by Persistent Scatterer Interferometry Measures and Landslide Inventories." *Remote Sensing* 4 (12): 1310–1336. doi:10.3390/rs4051310.

Hyde, P., R. Dubayah, W. Walker, J. B. Blair, M. Hofton, and C. Hunsaker. 2006. "Mapping Forest Structure for Wildlife Habitat Analysis Using Multi-Sensor (LiDAR, SAR/InSAR, ETM+, Quickbird) Synergy." *Remote Sensing of Environment* 102 (1–2): 63–73. doi:10.1016/j.rse.2006.01.021.

Im, J., J. R. Jensen, and J. A. Tullis. 2008. "Object-Based Change Detection Using Correlation Image Analysis and Image Segmentation." *International Journal of Remote Sensing* 29 (2): 399–423. doi:10.1080/01431160601075582.

Ivits, E., and B. Koch. 2002. "Object-Oriented Remote Sensing Tools for Biodiversity Assessment: A European Approach." In *Geoinformation for European-wide Integration: Proceedings of the 22nd Earsel Symposium*, edited by T. Benes. Rotterdam: Millpress, June 4–6. ISBN 90-77017-71-2.

Jeong, S. G., and C. H. Park. 2013. "Riparian Landcover Classification Using High Resolution Imagery and OOC Technique." In *13th International Multidisciplinary Scientific GeoConference: SGEM: Surveying Geology & mining Ecology Management*, 679–686. doi:10.5593/SGEM2013/BB2.V2/S10.018.

Kalliola, R., and K. Syrjänen. 1991. "To What Extent are Vegetation Types Visible in Satellite Imagery?" *Annales Botanici Fennici* 28 (1): 45–57. Finnish Zoological and Botanical Publishing Board. http://www.jstor.org/stable/23725347

Ke, Y., L. J. Quackenbush, and J. Im. 2010. "Synergistic Use of Quickbird Multispectral Imagery and LIDAR Data for Object-Based Forest Species Classification." *Remote Sensing of Environment* 114: 1141–1154.

Keramitsoglou, I., C. Kontoes, N. Sifakis, J. Mitchley, and P. Xofis. 2005. "Kernel Based Re-Classification of Earth Observation Data for Fine Scale Habitat Mapping." *Journal for Nature Conservation* 13 (2–3): 91–99. doi:10.1016/j.jnc.2005.02.004.

Kim, B. J., D. H. Oh, S. H. Chun, and S. D. Lee. 2011. "Distribution, Density, and Habitat Use of the Korean Water Deer (Hydropotes Inermis Argyropus) in Korea." *Landscape and Ecological Engineering* 7 (2): 291–297. doi:10.1007/s11355-010-0127-y.

Kloiber, S. M., R. D. Macleod, A. J. Smith, J. F. Knight, and B. J. Huberty. 2015. "A Semi-Automated, Multi-Source Data Fusion Update of a Wetland Inventory for East-Central Minnesota, USA." *Wetlands* 35 (2): 335–348. doi:10.1007/s13157-014-0621-3.

Laliberte, A. S., E. L. Fredrickson, and A. Rango. 2007. "Combining Decision Trees with Hierarchical Object-Oriented Image Analysis for Mapping Arid Rangelands." *Photogrammetric Engineering & Remote Sensing* 73 (2): 197–207. doi:10.14358/PERS.73.2.197.

Laliberte, A. S., J. Koppa, E. L. Fredrickson, and A. Rango. 2006. "Comparison of Nearest Neighbor and Rule-Based Decision Tree Classification in an Object-Oriented Environment." IEEE International Conference on Geoscience and Remote Sensing Symposium, Denver, CO, July 31–August 4.

Lu, D., P. Mausel, E. Brondízio, and E. Moran. 2004. "Relationships between Forest Stand Parameters and Landsat TM Spectral Responses in the Brazilian Amazon Basin." *Forest Ecology and Management* 198 (1–3): 149–167. doi:10.1016/j.foreco.2004.03.048.

Mallinis, G., N. Koutsias, M. Tsakiri-Strati, and M. Karteris. 2008. "Object-Based Classification Using Quickbird Imagery for Delineating Forest Vegetation Polygons in a Mediterranean Test Site." *ISPRS Journal of Photogrammetry and Remote Sensing* 63 (2): 237–250. doi:10.1016/j.isprsjprs.2007.08.007.

Marcus, W. A., R. A. Marston, C. R. Colvard, and R. D. Gray. 2002. "Mapping the Spatial and Temporal Distributions of Woody Debris in Streams of the Greater Yellowstone Ecosystem, USA." *Geomorphology* 44 (3–4): 323–335. doi:10.1016/S0169-555X(01)00181-7.

McKenna, J. E.Jr, and C. Castiglione. 2010. "Hierarchical Multi-Scale Classification of Nearshore Aquatic Habitats of the Great Lakes: Western Lake Erie." *Journal of Great Lakes Research* 36 (4): 757–771. doi:10.1016/j.jglr.2010.09.005.

Melese, D., K. V. Suryabhagavan, M. Gelet, and M. Balakrishnan. 2014. "Remote Sensing and Geographic Information System-Based African Civet Habitat Mapping in Andracha, Ethiopia." *Journal of Applied Remote Sensing* 8 (1): 83502. doi:10.1117/1.JRS.8.083502.

Moffett, K. B., and S. M. Gorelick. 2013. "Distinguishing Wetland Vegetation and Channel Features with Object-Based Image Segmentation." *International Journal of Remote Sensing* 34 (4): 1332–1354. doi:10.1080/01431161.2012.718463.

Mücher, C. A., L. Roupioz, H. Kramer, M. M. B. Bogers, R. H. G. Jongman, R. M. Lucas, V. E. Kosmidou, Z. Petrou, I. Manakos, E. Padoa-Schioppa, M. Adamo, and P. Blonda. 2015. "Synergy of Airborne LiDAR and Worldview-2 Satellite Imagery for Land Cover and Habitat Mapping: A BIO_SOS-EODHaM Case Study for the Netherlands." *International Journal of Applied Earth Observation and Geoinformation* 37: 48–55. doi:10.1016/j.jag.2014.09.001.

Naiman, R. J., and H. Décamps. 1997. "The Ecology of Interfaces: Riparian Zones." *Annual Review of Ecology and Systematics* 28: 621–658. doi:10.1146/annurev.ecolsys.28.1.621.

Nelson, R., W. Krabill, and J. Tonelli. 1988. "Estimating Forest Biomass and Volume Using Airborne Laser Data." *Remote Sensing of Environment* 24 (2): 247–267. doi:10.1016/0034-4257(88)90028-4.

Nie, Y., Y. Zhang, L. Liu, and J. Zhang. 2010. "Glacial Change in the Vicinity of Mt. Qomolangma (Everest), Central High Himalayas since 1976." *Journal of Geographical Sciences* 20 (5): 667–686. doi:10.1007/s11442-010-0803-8.

Norman, D. 2012. "The Detection of Forest Structures in the Monongahela National Forest Using LiDAR." Theses, Dissertations and Capstones. Paper 258. http://mds.marshall.edu/etd/258

Ouyang, Z.-T., M.-Q. Zhang, X. Xie, Q. Shen, H.-Q. Guo, and B. Zhao. 2011. "A Comparison of Pixel-Based and Object-Oriented Approaches to VHR Imagery for Mapping Saltmarsh Plants." *Ecological Informatics* 6 (2): 136–146. doi:10.1016/j.ecoinf.2011.01.002.

Pal, M., and P. M. Mather. 2003. "An Assessment of the Effectiveness of Decision Tree Methods for Land Cover Classification." *Remote Sensing of Environment* 86 (4): 554–565. doi:10.1016/S0034-4257(03)00132-9.

Patil, D. V., and R. S. Bichkar. 2006. "A Hybrid Evolutionary Approach to Construct Optimal Decision Trees with Large Data Sets." In *IEEE International Conference on Industrial Technology, 2006. ICIT 2006*, 429–433. IEEE.

Pekkarinen, A. 2002. "A Method for the Segmentation of Very High Spatial Resolution Images of Forested Landscapes." *International Journal of Remote Sensing* 23 (14): 2817–2836. doi:10.1080/01431160110076162.

Pierce, A. D., C. A. Farris, and A. H. Taylor. 2012. "Use of Random Forests for Modeling and Mapping Forest Canopy Fuels for Fire Behavior Analysis in Lassen Volcanic National Park, California, USA." *Forest Ecology and Management* 279: 77–89. doi:10.1016/j.foreco.2012.05.010.

Qian, J., Q. Zhou, and Q. Hou. 2007. "Comparison of Pixel-Based and Object-Oriented Classification Methods for Extracting Built-up Areas in Arid Zone." In *ISPRS Workshop on Updating Geo-Spatial Databases with Imagery & The 5thISPRSWorkshoponDMGISs*, 163–171. http://www.isprs.org/proceedings/XXXVI/4-W54/papers/163-171.pdf

Radoux, J., and P. Defourny. 2007. "A Quantitative Assessment of Boundaries in Automated Forest Stand Delineation Using Very High Resolution Imagery." *Remote Sensing of Environment* 110 (4): 468–475. doi:10.1016/j.rse.2007.02.031.

Rapinel, S., L. Hubert-Moy, and B. Clément. 2014. "Combined Use of LiDAR Data and Multispectral Earth Observation Imagery for Wetland Habitat Mapping." *International Journal of Applied Earth Observation and Geoinformation*. doi:10.1016/j.jag.2014.09.002.

Rhim, S.-J., and W.-S. Lee. 2007. "Influence of Forest Fragmentation on the Winter Abundance of Mammals in Mt. Chirisan National Park, South Korea." *Journal of Wildlife Management* 71 (5): 1404–1408. doi:10.2193/2005-584.

Rodríguez, D., F. Cuesta, I. Goldstein, L. G. Naranjo, O. L. Hernández, and A. E. Bracho. 2003. Ecoregional Strategy for the Conservation of the Spectacled Bear (Tremarctos Ornatus) in the

Northern Andes. World Wildlife Fund, Fundación Wii, EcoCiencia, Wildlife Conservation Society and Red Tremarctos.

Rodriguez-Iturbe, I., R. Muneepeerakul, E. Bertuzzo, S. A. Levin, and A. Rinaldo. 2009. "River Networks as Ecological Corridors: A Complex Systems Perspective for Integrating Hydrologic, Geomorphologic, and Ecologic Dynamics." *Water Resources Research* 45. doi:10.1029/2008wr007124.

Rönnholm, P., J. Hyyppä, H. Hyyppä, H. Haggrén, X. Yu, and H. Kaartinen. 2004. "Calibration of Laser-Derived Tree Height Estimates by Means of Photogrammetric Techniques." *Scandinavian Journal of Forest Research* 19 (6): 524–528. doi:10.1080/02827580410019436.

Ruiz-Olmo, J., J. M. López-Martín, and S. Palazón. 2001. "The Influence of Fish Abundance on the Otter (Lutra Lutra) Populations in Iberian Mediterranean Habitats." *Journal of Zoology* 254 (3): 325–336. doi:10.1017/S0952836901000838.

Saura, S., and L. Pascual-Hortal. 2007. "A New Habitat Availability Index to Integrate Connectivity in Landscape Conservation Planning: Comparison with Existing Indices and Application to a Case Study." *Landscape and Urban Planning* 83 (2–3): 91–103. doi:10.1016/j.landurbplan.2007.03.005.

Scorpio, V., A. Loy, M. Di Febbraro, A. Rizzo, and P. Aucelli. 2014. "Hydromorphology Meets Mammal Ecology: River Morphological Quality, Recent Channel Adjustments and Otter Resilience." *River Research and Applications*. Wiley Online Library. doi:10.1002/rra.2848.

Simard, M., G. De Grandi, S. Saatchi, and P. Mayaux. 2002. "Mapping Tropical Coastal Vegetation Using JERS-1 and ERS-1 Radar Data with a Decision Tree Classifier." *International Journal of Remote Sensing* 23 (7): 1461–1474. doi:10.1080/01431160110092984.

Smeeckaert, J., C. Mallet, N. David, N. Chehata, and A. Ferraz. 2013. "Large-Scale Classification of Water Areas Using Airborne Topographic Lidar Data." *Remote Sensing of Environment* 138: 134–148. doi:10.1016/j.rse.2013.07.004.

Smith, J. H., J. D. Wickham, S. V. Stehman, and L. Yang. 2002. "Impacts of Patch Size and Land-Cover Heterogeneity on Thematic Image Classification Accuracy." *Photogrammetric Engineering and Remote Sensing* 68: 65–70.

Soulé, M. E., and J. Terborgh. 1999. "Conserving Nature at Regional and Continental Scales—A Scientific Program for North America." *BioScience* 49 (10): 809–817. doi:10.2307/1313572.

Stevens, S. S., J. F. Organ, and T. L. Serfass. 2011. "Otters as Flagships: Social and Cultural Considerations." In *Proceedings of Xth International Otter Colloquium*, vol. 28, 150–161. IUCN/SCC Otter Specialist Group Bulletin.

Tehrany, M. S., B. Pradhan, and M. N. Jebuv. 2014. "A Comparative Assessment between Object and Pixel-Based Classification Approaches for Land Use/land Cover Mapping Using SPOT 5 Imagery." *Geocarto International* 29 (4): 351–369. doi:10.1080/10106049.2013.768300.

Tiede, D., S. Lang, F. Albrecht, and D. Hölbling. 2010. "Object-Based Class Modeling for Cadastre-Constrained Delineation of Geo-Objects. Photogramm." *Photogrammetric Engineering & Remote Sensing* 76: 193–202. doi:10.14358/PERS.76.2.193.

Todd, S. W., and R. M. Hoffer. 1998. "Responses of Spectral Indices to Variations in Vegetation Cover and Soil Background." *Photogrammetric Engineering and Remote Sensing* 64 (9): 915–922.

Treitz, P., and P. Howarth. 2000. "Integrating Spectral, Spatial, and Terrain Variables for Forest Ecosystem Classification." *Photogrammetric Engineering and Remote Sensing* 66 (3): 305–318.

Varela, R. A. D., P. R. Rego, S. C. Iglesias, and C. M. Sobrino. 2008. "Automatic Habitat Classification Methods Based on Satellite Images: A Practical Assessment in the NW Iberia Coastal Mountains." *Environmental Monitoring and Assessment* 144 (1–3): 229–250. doi:10.1007/s10661-007-9981-y.

Xiaofeng, L., Q. Yi, L. Diqiang, L. Shirong, W. Xiulei, W. Bo, and Z. Chunquan. 2011. "Habitat Evaluation of Wild Amur Tiger (Panthera Tigris Altaica) and Conservation Priority Setting in North-Eastern China." *Journal of Environmental Management* 92 (1): 31–42.

White, P. C. L., C. J. McClean, and G. L. Woodroffe. 2003. "Factors Affecting the Success of an Otter (Lutra Lutra) Reinforcement Programme, as Identified by Post-Translocation Monitoring." *Biological Conservation* 112 (3): 363–371. doi:10.1016/S0006-3207(02)00333-6.

Zhang, L., and X. Huang. 2010. "Object-Oriented Subspace Analysis for Airborne Hyperspectral Remote Sensing Imagery." *Neurocomputing* 73 (4–6): 927–936. doi:10.1016/j.neucom.2009.09.011.